Left Handed Metamaterial incorporate with Microstrip Antenna Array Design and Analysis

Huda A Majid and Mohamad Kamal A Rahim

Abstract— This paper describes and analyzes a new structure of left-handed metamaterial (LHM) which consists of a modified square rectangular split ring (MSRR) and a capacitance loaded strip (CLS) used to obtain LHM structure. Simulation and analysis was done using Computer Simulation Technology (CST) software. Parametric studies on the LHM structure were carried out and the effect of frequency and the range of negative value of permeability ($-\mu_r$) and the negative permittivity ($-\varepsilon_r$) were observed. The changes in the dimension of MSSR and CLS affect the S_{11} and S_{21} of the LHM structure and thus affect the value of permeability and the permittivity. The value of permeability and the permittivity was extracted from the reflection and transmission coefficient data using a Nicolson-Ross-Wier (NRW) approach. Studies proved that the LHM structure can be designed in the frequency range of interest. In order to prove the concept of LHM, an array of LHM is incorporated with a linear polarized 2x2 array patch antenna. The negative refraction index of LHM produces a focusing effect to the radiation of the antenna. Due to this effect, the gain of the antenna increases up to 2 dB and the 3 dB beamwidth becomes narrow.

Index Terms— Left-Handed Metamaterial, Negative Permittivity, Negative Permeability, Split Ring Resonator, Capacitance Loaded Strip, microstrip array antenna.

1 INTRODUCTION

LEFT – HANDED Metamaterial (LHM) is an electromagnetic metamaterial which exhibits negative permittivity and permeability in a certain frequency range [1]. This phenomenon can be characterized by the negative refraction index and backward wave. The backward wave propagation has been verified in [2] and the negative refraction has been proven in [3]. Many authors have proposed and published new structures that produced negative permittivity (ε_r) and permeability (μ_r) [4],[5],[6]. The first left-handed metamaterial in microwave range consist of the metallic wire and split ring resonator [7]. Metamaterial consisting of metallic mesh wire has been widely studied [8]. The structure, which has very small electric length in the period of wire thickness is characterized as a homogeneous medium with low plasma frequency and exhibits negative permittivity [8], [9]. At the same time, a split ring resonator has been proven to exhibit negative permeability over the microwave frequency band [10],[11]. The existence of both structures operating in the microwave frequency band has produced new ideas and created various new microwave applications. For example, a new method to improve the gain in rectangular and circular waveguide antenna arrays using double negative medium (DNG) structures consisting of strip wires and split ring resonators was proposed in [12-13]. Metamaterial superstrate consisting of stacked S-shaped split ring resonators were designed at WiMAX 2.5 GHz band [14]. An E-plane horn antenna incorporated with metamaterial made up of metallic cylinders organized in a two-dimensional square lattice produced directional beam pattern in four different directions [15]. In this research, parametric study on a new structure of LHM has been undertaken to analyze the effect of resonant frequency and the value of ε_r and μ_r. It consists of one MSRR between two pairs of CLSs in planar form. MSRR exhibits a negative value of permeability while CLS exhibits a negative value of permittivity.

Figure 1 shows the initial design of the LHM unit cells proposed by Ziolkowski [16]. As can be seen, the LHM structure has four CLSs and a single SRR, and it is placed in a substrate with a dielectric constant of 2.2. The dimension of LHM unit cell structure is 4.318 mm high, 2.3622 mm wide and 7.366 mm long

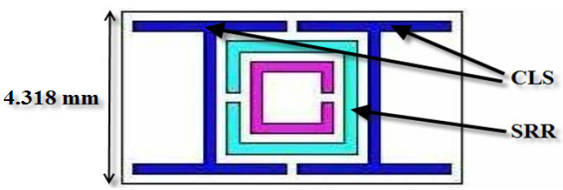

(a)

- *Huda A Majid is a PhD research student at Universiti Teknologi Malaysia Johor Bahru Malaysia.*
- *Mohamad Kamal A Rahim is with the Radio Communication Engineering Department, Faculty of Electrical Engineering, Universiti Teknologi Malaysia Johor Bahru Malaysia.*

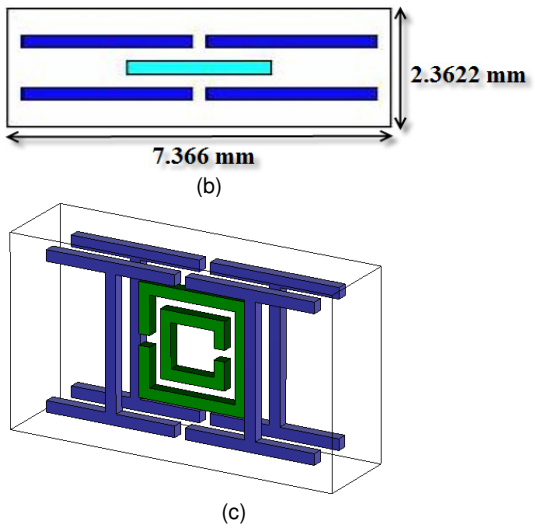

Fig. 1 (a) side view of the LHM (b) top view of the LHM and (c) perspective view of the LHM proposed by Ziolkowski [14]

In order to use less substrate and reduce the cost of the project, a planar structure is proposed in the design of LHM. The new design of LHM structure is shown in Figure 2 and consists of two CLSs and a SRR [17].

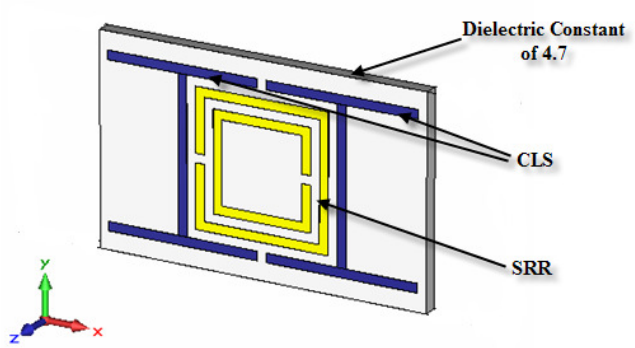

Fig. 2 Proposed LHM structure

A few modifications on the SRR have been made in order to analyze the effect of permittivity and permeability. Figures 3 to 6 show the proposed LHM structure where the SRR of the structure is modified. The first LHM structure is the initial structure design by Ziolkowski, while the second LHM structure is modified in such a way that the SRR has four gaps and the gaps are placed at the centre of the structure. The SRR of the third LHM structure also has four gaps and the gaps are placed perpendicular to the structure, while the SRR of the fourth LHM structure has eight gaps.

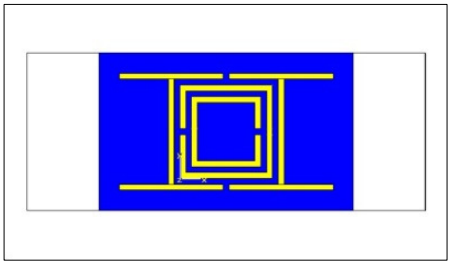

Fig. 3 First Left Handed Metamaterial Structure

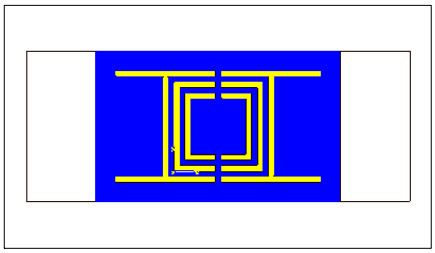

Fig. 4 Second Left Handed Metamaterial Structure

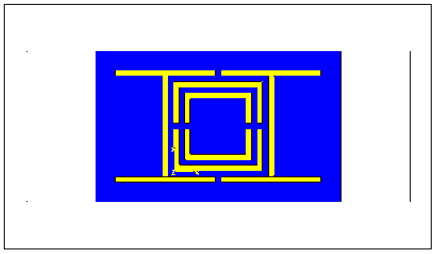

Fig. 5 Third Left handed Metamaterial Structure

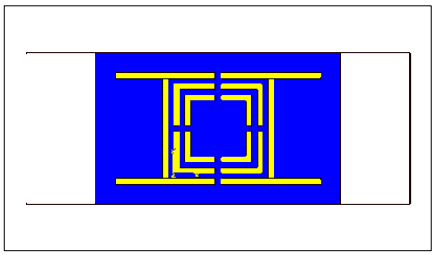

Fig. 6 Fourth left handed Metamaterial Structure

In order to improve new design structures from Ziolkowski, the initial design will be neglected from the analysis. The second proposed LHM structure shown in Figure 4 has a wide band of negative ε_r and μ_r from 4.08 GHz to 4.67 GHz respectively and the third proposed LHM structure shown in Figure 5 also has a wide band of negative ε_r and negative μ_r from 3.50 GHz to 4.02 GHz respectively. The fourth LHM structure from Figure 6 has an almost non-existing band of negative ε_r and negative μ_r.

Subsequently, the only structures that can be chosen are the second and third proposed structures. Although the second proposed structure is operating at higher frequency than the third proposed structure, it has been chosen for further analysis because the second proposed structure has a wider frequency range of negative ε_r and μ_r compared to the third proposed structure. The initial dimension of the LHM unit cell is shown in Figure 7. It consists of one SRR between two pairs of CLSs in planar form. Table 1 shows the dimensions of the LHM. The dielectric constant of the substrate is 4.7, with a thickness of 1.6 mm and a tangential loss of 0.019.

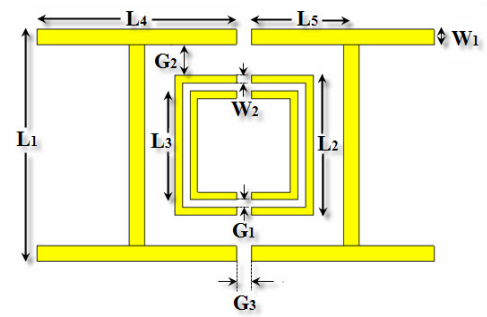

Fig. 7 The dimension of Left Handed Metamaterial

TABLE 1
DIMENSION OF LHM

Parameters	Dimension (mm)
W_1	1.0
W_2	0.5
G_1	0.5
G_2	2.0
G_3	1.0
L_1	15.1
L_2	9.1
L_3	7.1
L_4	13.1
L_5	6.55

2 Determination of Permittivity and Permeability using Modified Nicolson-Ross Wier (NRW) Approach

In order to get a more accurate approximation of the permittivity and permeability, the modified NRW Approach was applied in this research [10]. NRW approach is a commonly used technique to determine the value of permittivity and permeability.

$$\mu_r \approx \frac{2}{jk_0 d}\frac{1-V_2}{1+V_2} \qquad (1.0)$$

$$\varepsilon_r \approx \frac{2}{jk_0 d}\frac{1-V_1}{1+V_1} \qquad (2.0)$$

Where: d = thickness of substrate

$$k_0 = \frac{\omega}{c}$$

$$V_2 = S_{21} - S_{11}$$

$$V_1 = S_{21} + S_{11}$$

Equation 1.0 and 2.0 are used to calculate the permittivity and permeability of the LHM. This was done by exporting the S-Parameters from CST Microwave Studio software to MathCAD software.

3 Boundary Condition for Simulation Set Up

The simulation of LHM has been done using Computer Simulation Technology (CST) software. A Perfect magnetic conductor (PMC) boundary condition is set on the front and back faces of the block in z-axis and a perfect electric conductor (PEC) boundary condition is set on the top and bottom of the block in the y-axis. The E-field of the incident wave is polarized along the y-axis while the H-field of the incident wave is polarized along the z-axis and the wave propagates in x direction. Figure 8 illustrates the simulated structure.

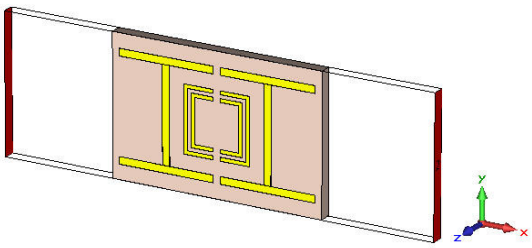

Fig. 8 Boundary condition for simulation setup

Through this configuration, the S-Parameters (S_{11} and S_{21}) data are collected and exported to MathCAD for calculation of the LHM region using the modified NRW Approach [5]. Consequently, two parameters of the unit cell (L_2 and G_2) are varied in order to study the influence of the resonant frequency and the value of ε_r and μ_r

4 Parametric Studies and Analysis of Left Handed Metamaterial Unit Celll

4.1 Varying the Gap between the MSRR and the CLS, G_2

In this case, the gap between the MSRR and the CLS [G_2] is varied to observe the effect of the resonant frequency and the value of ε_r and μ_r. The dimension of the MSRR is fixed as an initial structure shown in Figure 7. The results are plotted and shown in Figure 9 and Table 2.

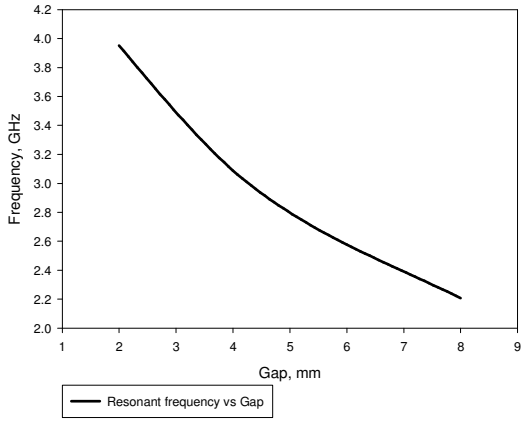

Fig. 9 Correlation between gap, G_2 and resonant frequency

Referring to Figure 9, the resonant frequency is shifted by varying the gap, G_2. When the gap, G_2 increases, the resonant frequency reduces, while the range of negative ε_r and negative μ_r is shifted to the lower region as shown in Table 2. Note that, by varying the gap between the SRR and CLS, G_2 the CLS inclusion, L_1 and CLS length, L_4 also varies. Table 3 shows the correlation between the gap, G_2 and CLS inclusion, L_1. Meanwhile, Table 4 shows the correlation between the gap, G_2 and the CLS length, L_4.

TABLE 2
CORRELATION BETWEEN FREQUENCY RANGE OF NEGATIVE PERMITTIVITY, ε_r AND NEGATIVE PERMEABILITY , μ_r WITH GAP, G_2

Gap (G_2)	Frequency range of negative permittivity & permeability (GHz)
2 mm	4.000 - 4.224
4 mm	3.104 - 3.264
6 mm	2.592 - 2.736
8 mm	2.224 - 2.336

TABLE 3
CORRELATION BETWEEN GAP,G_2 AND LENGTH, L_1

Gap (G_2)	CLS inclusion length (L_1)
2 mm	15.1 mm
4 mm	19.1 mm
6 mm	23.1 mm
8 mm	27.1 mm

TABLE 4
CORRELATION BETWEEN GAP, G_2 AND LENGTH, L_4

Gap (G_2)	CLS strip length (L_4)
2 mm	13.1 mm
4 mm	17.1 mm
6 mm	21.1 mm
8 mm	25.1 mm

4.2 Varying the Length of outer MSRR, L_2

In this simulation, the length of the outer MSRR [L_2] is varied to observe the effect of the resonant frequency and the value of ε_r and μ_r. As the L_2 is varied, other parameters such as L_1, L_3 and L_4 are altered as those parameters are related to L_2

Figure 10 shows the correlation between L_2 and the resonant frequency. As the length of the outer MSRR increases, the resonant frequency goes to the lower region. Consequently, the range of negative ε_r and μ_r also goes to the lower frequency region as the value of L_2 increases as shown in Table 5. As a result on varying the value of L_2, other parameters also are altered. Table 6 shows the correlation between the MSRR outer length, L_2 with the MSRR inner length, L_3. Table 7 shows the correlation between MSRR outer length, L_2 with the CLS inclusion length, L_1. While, Table 8 shows the relationship between the MSRR outer length, L_2 with the CLS strip length, L_4. As can be seen from these three tables, the value of L_3, L_1 and L_4 increase as the MSRR outer length L_2 increases. This shows that increasing the size of the structure will make the resonant frequency and the range of negative ε_r and μ_r shift to the lower region.

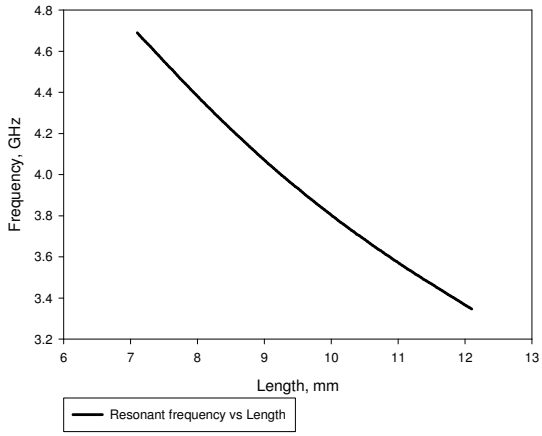

Fig. 10 Correlation between length, L_2 and resonant frequency

TABLE 5
CORRELATION BETWEEN FREQUENCY RANGE OF NEGATIVE PERMITTIVITY, ε_r AND NEGATIVE PERMEABILITY, μ_r WITH LENGTH, L_2

MSRR outer length (L_2)	Frequency range of negative permittivity & permeability (GHz)
7.1 mm	4.762 - 4.936
8.1 mm	4.426 - 4.552
9.1 mm	4.084 - 4.264
10.1 mm	3.808 - 4.036
11.1 mm	3.568 - 3.808
12.1 mm	3.358 - 3.736

TABLE 6
CORRELATION BETWEEN LENGTH, L_2 AND L_3

MSRR outer length (L_2)	MSRR inner length (L_3)
7.1 mm	5.1 mm
8.1 mm	6.1 mm
9.1 mm	7.1 mm
10.1 mm	8.1 mm
11.1 mm	9.1 mm
12.1 mm	10.1 mm

TABLE 7
CORRELATION BETWEEN LENGTH, L_2 AND L_1

MSRR outer length (L_2)	CLS inclusion length (L_1)
7.1 mm	13.1 mm
8.1 mm	14.1 mm
9.1 mm	15.1 mm
10.1 mm	16.1 mm

11.1 mm	17.1 mm
12.1 mm	18.1 mm

TABLE 8
CORRELATION BETWEEN LENGTH, L_2 AND L_4

MSRR outer length (L_2)	CLS strip length (L_4)
7.1 mm	11.1 mm
8.1 mm	12.1 mm
9.1 mm	13.1 mm
10.1 mm	14.1 mm
11.1 mm	15.1 mm
12.1 mm	16.1 mm

4.3 Varying the Width of CLS, W_1

In this case, the width of the CLS, W_1 is varied to observe the effect to the resonant frequency and the value of permittivity and permeability. The diagram in Figure 11 shows that when the parameter becomes larger, the resonant frequency becomes lower, which also affects the frequency range of ε_r and μ_r as shown in Table 9. The frequency range of negative permittivity and permeability shift to the lower region as the width of the CLS [W_1] increases.

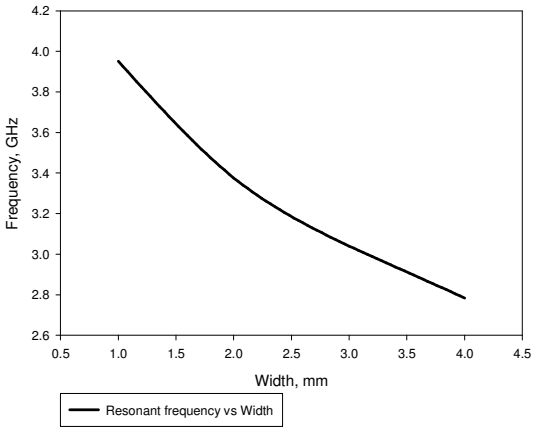

Fig. 11 Correlation between width, W_1 and resonant frequency

TABLE 9
CORRELATION BETWEEN FREQUENCY RANGE OF NEGATIVE PERMITTIVITY, ε_r AND NEGATIVE PERMEABILITY, μ_r WITH WIDTH, W_1

Width (W_1)	Frequency range of negative permittivity & permeability (GHz)
1 mm	4.0 - 4.224
2 mm	3.392 - 4.016
3 mm	3.04 - 4.048
4 mm	2.784 - 3.744

4.4 Varying the Gaps [G_1] and Width [W_2] of MSRR

The gaps, G_1 and width, W_2 of the MSRR are varied from 0.5 to 1.25 mm for both gap and width respectively.

It was observed that the gap, G_1 and width, W_2 did not have any significance to the resonant frequency and the values of ε_r and μ_r as shown in Figure 12 and Figure 13 respectively. In this case, both parameters have been varied and other parameter's dimensions were unchanged.

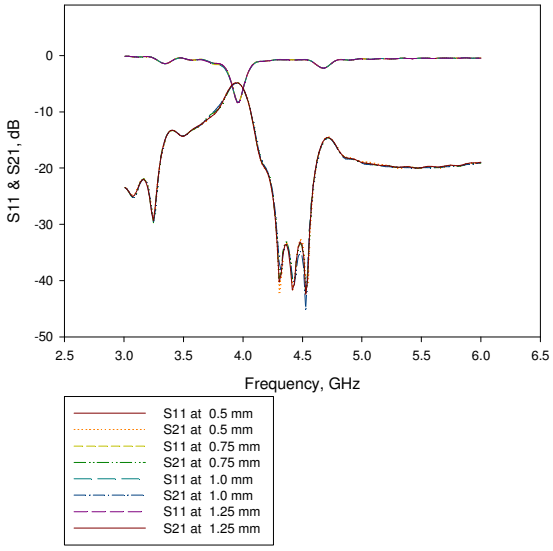

Fig. 12 Results of S_{11} and S_{21} of the LHM

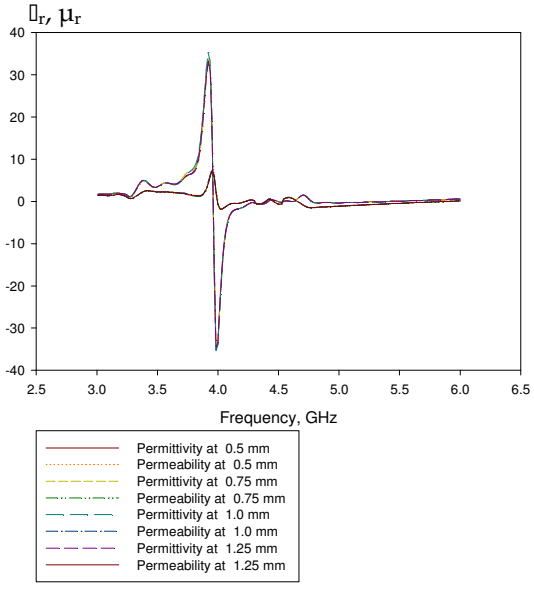

Fig. 13 Value of ε_r and μ_r

5 ANALYSIS OF LINEAR POLARIZED 2 X 2 ARRAY PATCH ANTENNA INCORPORATED WITH LHM

In order to prove that the LHM structure is working, an array of LHM is placed in front of a linear polarized 2x2 array patch antenna. The effects of the integration of LHM to the parameters of the antenna are discussed and analyzed. Figure 14 illustrates the LHM incorporated with the antenna. An array of LHM is arranged with an air gap of 8 mm between each LHM cells while the gap between the LHM and the antenna is 12.5 mm. Figure 15 shows the comparison of S_{11} measured results for both antennas with and without LHM. The comparison of S_{21} measured results for both antennas with and without LHM is shown in Figure 16

Fig. 14 Array of LHM incorporated with linear polarized 2x2 array patch antenna

As can be seen from figure 15, the resonant frequency is shifted to a higher frequency region from 2.43 GHz to 2.48 GHz. The resonant frequency at 2.4 GHz before the placement of the LHM is -10.2 dB and -7.6 dB after the LHM is placed in front of the antenna. Although the return loss is slightly degraded, the result of S_{21} from figure 16 shows an increment in magnitude up to 2 dB at 2.4 GHz. In other words, the focusing effect of the LHM is still operating at 2.4 GHz even though the return loss at that frequency is degraded. Above 2.52 GHz, the transmission coefficient reduced to the lower value and acted similar to a stop band after the incorporation of the LHM.

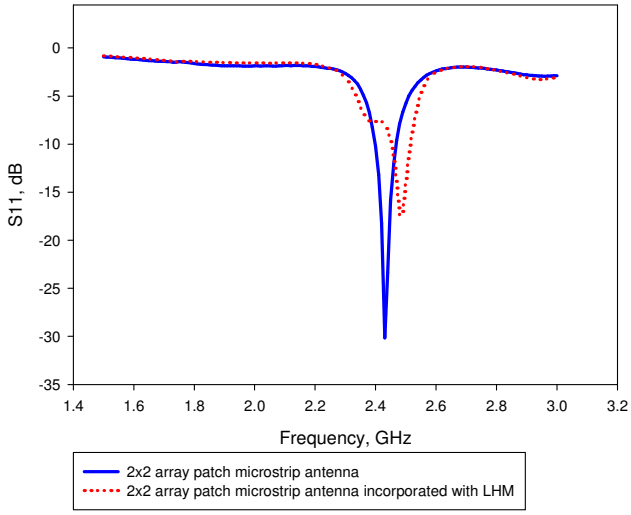

Fig. 15 Return loss, S_{11} of the linear polarized 2x2 Array Patch Microstrip Antenna Incorporated with and without LHM

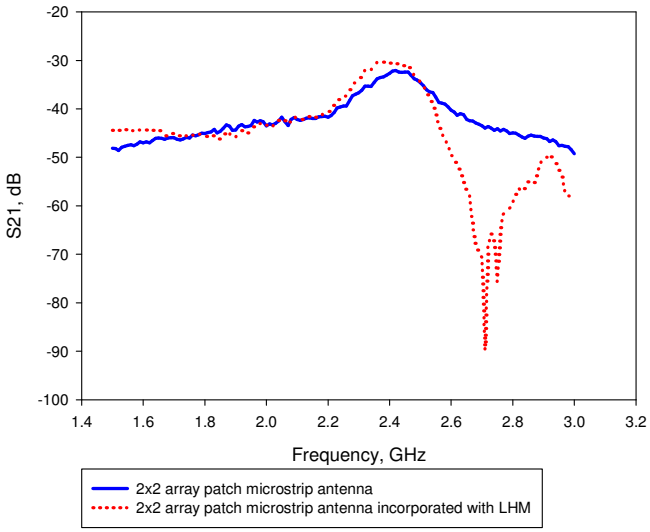

Fig. 16 Transmission coefficient, S_{21} of the linear polarized 2x2 Array Patch Microstrip Antenna Incorporated with and without LHM

The radiation pattern of the antenna with and without LHM is measured in order to prove the focusing effect of the LHM. Figure 17 shows the radiation pattern for both antennas, with and without LHM in E-plane at the frequency of 2.4 GHz. The 3 dB beam-width of the antenna incorporated with LHM is 48^0 similar compared to the antenna without the LHM. From Figure 18, the 3 dB beam-width for H-plane changes from 44^0 to 38^0 after incorporating the LHM to the antenna. The front to back ratio and front to side ratio show similarity values for both antennas with and without LHM.

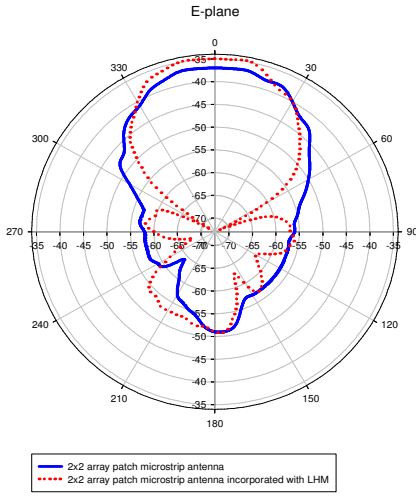

Fig. 17 Measured radiation pattern in E-plane

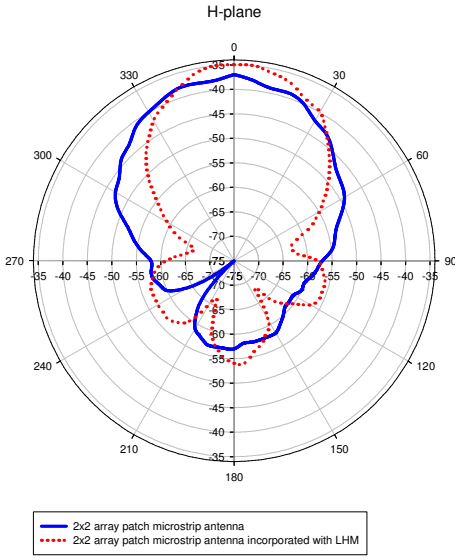

Fig. 18 Measured radiation pattern in H-plane

Figure 19(a) and 19(b) shows the radiation pattern of the antenna incorporated with LHM for both simulated and measured. Both results correlate well with each other where the shapes of the radiation patterns are concerned. It shows that when antenna is incorporated with the left handed metamaterial the beamwidth of the antenna becomes narrower. The directivity of the antenna has been increased. Left handed metamaterial has increased the gain of the antenna by 2 dB. The halfpower beamwidth of the antenna is reduced for H plane while the Eplane maintained the same halfpower beamwidth.

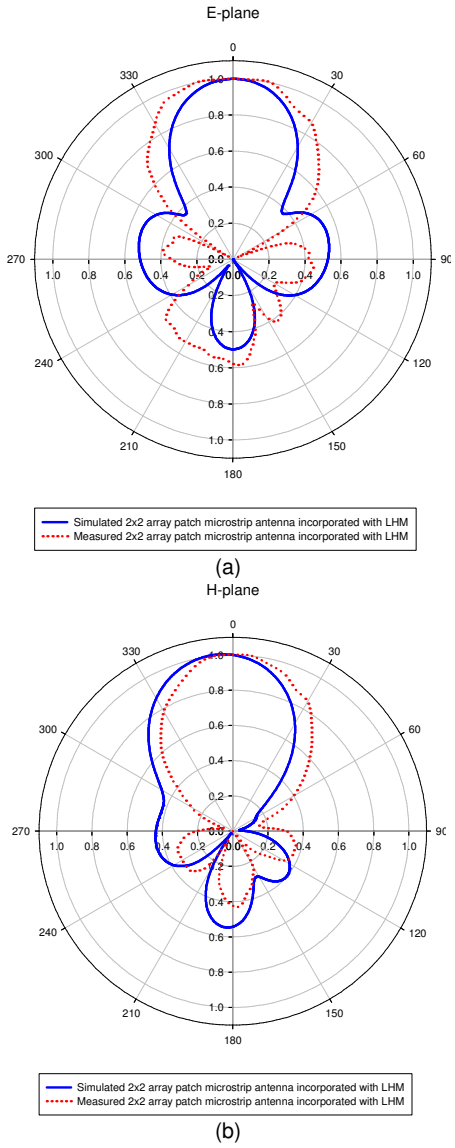

Fig. 19 (a) Comparison between simulated and measured radiation patterns in E-plane and (b) Comparison between simulated and measured radiation patterns in H-plane

6 Discussion

From observation, there are some parameters that have a very strong influence to the resonant frequency, whilst others are not significant. As examples, the gap, G_1 and width, W_2 is varied from 0.5 mm to 1.25 mm. From observation, the resonant frequency and the frequency range of negative ε_r and μ_r did not shift as the parameters varied. This is due to the small variation of steps used in the study. If larger steps are used, the resonant frequency and the frequency range of negative ε_r and μ_r will shift. The gap G_2 is varied form 2 mm to 8 mm. This shifts the resonant frequency from 4 GHz to 2.2 GHz. The frequency range of negative ε_r and μ_r is also shifted from 4 GHz to 2.2 GHz. The variation of G_2 also varies other parameters, such as the length L_1 and L_4. The resonant frequency is shifted from 4.7 GHz to 3.3 GHz linearly after the length

L_2 is varied. The frequency range of negative ε_r and μ_r is also shifted with a similar range to the resonant frequency. The variation of L_2 also varies with other parameters such as the length, L_1, L_3 and L_4. The width W_1 is varied from 1 mm to 4 mm and this shifts the resonant frequency from 3.9 GHz to 2.8 GHz. The frequency range of negative ε_r and μ_r is also shifted from 4.2 GHz to 2.7 GHz.

The LHM structure which operates at 2.4 GHz has been chosen to be incorporated with a 2.4 GHz linear polarized 2x2 array patch antenna. In order to make it more clearer, comparison of the antenna's parameter between linear polarized 2x2 array patch microstrip antenna with and without LHM is presented in Table 10.

TABLE 10
COMPARISON OF THE ANTENNA'S PERFORMANCE BETWEEN LINEAR POLARIZED 2 X 2 ARRAY PATCH ANTENNA WITH AND WITHOUT LEFT HANDED METAMATERIAL

Antenna parameters at 2.4 GHz		Linear polarized 2x2 array patch microstrip antenna	Linear polarized 2x2 array patch microstrip antenna incorporated with LHM
Return loss, S_{11}		-10.2 dB	-7.6 dB
Power Received		-33 dBm	-31 dBm
Bandwidth		2.3 % (2.395 GHz – 2.45 GHz)	2.8 % (2.45 GHz – 2.52 GHz)
Gain		0 dB	2 dB
3dB beam-width	E-plane	48^0	48^0
	H-plane	44^0	38^0
Cross polar isolation	E-plane	36 dB	43 dB
	H-plane	32 dB	45 dB
Front to back lobe ratio		14 dB	16 dB

From Table 11, the simulated return loss S_{11} bandwidth and the 3 dB beam-width are almost similar to the measured one. The increment of the gain is also similar for simulated and measured and the other performances were different due to imperfections in the fabrication process

TABLE 11
COMPARISON BETWEEN SIMULATED AND MEASURED LINEAR POLARIZED 2 X 2 ARRAY PATCH ANTENNA INCORPORATED WITH LEFT HANDED METAMATERIAL

Antenna parameters at 2.4 GHz		Simulated linear polarized 2x2 array patch microstrip antenna incorporated with LHM	Measured linear polarized 2x2 array patch microstrip antenna incorporated with LHM
Return loss, S_{11}		-10 dB	-7.6 dB
Bandwidth		2.4 % (2.4 GHz – 2.46 GHz)	2.8 % (2.45 GHz – 2.52 GHz)
Gain increment		2.44 dB	2 dB
3dB beam-width	E-plane	42.1^0	48^0
	H-plane	38.2^0	38^0
Front to back lobe ratio		13.87 dB	16 dB

7 CONCLUSIONS

In conclusion, the parameters of G_2, L_2 and L_1 have strong influence in the resonant frequency and the frequency range of the negative value of ε_r and μ_r. The parameters of G_2, L_2 and L_1 play important roles as they denote the capacitance and inductance values that determine the operating frequencies of the structures. If a large change in the resonant frequency needed, these three parameters should be varied accordingly. Further works are needed to observe other parameters of LHM for their influence on the resonant frequencies and values of ε_r and μ_r. It is predicted that other parameters would also produce similar results as G_2 and L_2. The incorporation of LHM structures with an antenna shows that the LHM acts as focusing device where the gain of the antenna increases up to 2 dB and the 3 dB beamwidth becomes narrow. The bandwidth percentage of the antenna is also increases from 2.3 % to 2.8 %

ACKNOWLEDGMENT

The authors thank the Ministry of Higher Education (MOHE) for supporting the research work, Research Management Centre (RMC) and Radio Communication Engineering Department (RACeD), Universiti Teknologi Malaysia (UTM) for the support of the research

REFERENCES

[1] Christophe Caloz and Tatsuo Itoh, Electromagnetic Metamaterials Transmission Line Theory and Microwave Applications, John Wiley & Sons, Inc. 2006

[2] Jorge Carbonell, Luis J. Rogla, Vicente E. Boria, Didier Lippens, "Design and Experimental Verification of Backward-Wave Propagation in Periodic Waveguide Structures," *IEEE Transactions on Microwave Theory and Techniques*. Vol. 54, No. 4, 4 April 2006

[3] A. Aydin, G. Kaan and O Ekmel, "Two-Dimensional Left-handed Metamaterial with a Negative Refractive Index," *Journal of Physics.* Conference Series 36, 2006.

[4] B.-I. Wu, W. Wang, J. Pacheco, X. Chen, T. Grzegorczyk and J. A. Kong, "A Study of Using Metamaterials as Antenna Substrate to Enhance Gain," *Progress In Electromagnetics Research*, PIER 51, 295-328, 2005.

[5] X. Cheng, H. Chen, L. Ran, B. Wu, T. M. Grzegorczyk and J. A. Kong, "A Bianisotropic Left-handed Metamaterials Compose of S-ring Resonator," *PIERS Online*, Vol. 3, No. 5, 2007.

[6] F. Bilotti, A. Toscano and L. Vegni, "Design of Spiral and Multiple Split-Ring Resonators for the Realization of Miniatured Metamaterial Samples," *IEEE Transactions on Antennas and Propagatio,* Vol. 55, No. 8, August 2007.

[7] Shelby, R. A., D. R. Smith, and S. Schultz, "Experimental verification of a negative index of refraction," *Science*, Vol. 292, 77-79, Apr. 2001.

[8] Pendry, J. B., A. J. Holden, D. J. Robbins, and W. J. Stewart," Low frequency plasmons in thin-wire structures," *J. Phys. Condens. Matter*, Vol. 10, No. 22, 4785-4809, 1998.

[9] Hudlicka, M., J. Machac, and I. S. Nefedov, "A triple wire medium as an isotropic negative permittivity metamaterial," *Progress In Electromagnetics Research*, PIER 65, 233-246, 2006.

[10] Pendry, J. B., A. J. Holden, D. J. Robbins, and W. J. Stew- art, "Magnetism from conductors and enhanced nonlinear phenomena," *IEEE Trans. Microwave Theory Tech.*, Vol. 47, No. 11, 2075-2084, Nov. 1999.

[11] Xi, S., H. Chen, B.-I. Wu, and J. A. Kong, "Experimental confirmation of guidance properties using planar anisotropic left-handed metamaterial slabs based on S-Ring Resonators," *Progress In Electromagnetics Research*, PIER 84, 279-287, 2008.

[12] Liang, L., B. Li, S. H. Liu, and C. H. Liang, "A study of using the double negative structure to enhance the gain of rectangular waveguide antenna arrays," *Progress In Electromagnetics Research*, PIER 65, 275-286, 2006.

[13] Li, B., B. Wu, and C.-H. Liang, "Study on high gain circular waveguide array antenna with metamaterial structure," *Progress In Electromagnetics Research*, PIER 60, 207-219, 2006.

[14] Lin, H.-H., C.-Y. Wu, and S.-H. Yeh, "Metamaterial enhanced high gain antenna for WiMAX application," *IEEE AP-S*, Oct. 2007.

[15] R.-B. Hwang, H.-W. Liu, and C.-Y. Chin, "A Metamaterial-Based E-Plane Horn Antenna," *Progress In Electromagnetics Research*, PIER 93, 275-289, 2009.

[16] Richard W. Ziolkowski, "Design, Fabrication, and Testing of Double Negative Metamaterials," *IEEE Transactions on Antennas and Wireless Propagation*, Vol. 51, No. 7, 2003.

[17] H.A. Majid, M.K.A.Rahim, T. Masri. 2009. " Micrsotrip Antenna's Gain Enhancement using Left Handed Metamaterial structure", Progress in Electromagnetic Research M, vol 8, pp 235 – 247, 2009.

Huda A Majid received the B. Eng desgree in Telecommunication Engineering in 2007 and Master Engineering in Electrical in 2010 from Universiti Teknologi Malaysia. Currently he is a PhD Research student at Faculty of Electrical Engineering , Universiti Teknologi Malaysia. His research interest are left handed metamaterial, planar antenna, textile antenna and antenna for cognitive radio system.

Mohamad Kamal A Rahim received the B Eng degree in Electrical and Electronic Engineering from University of Strathclyde, UK in 1987. He obtained his Master Enginerring from University of New south Wales Australia in 1992. He graduated his PhD in 2003 from University of Birmingham U.K.in the field of Wideband Active Antenna. From 1992 to 1999, he was a lecturer at the Faculty of Engineering, Universiti Teknologi Malaysia. From 2005 to 2007, he was a senior lecturer at the Departmen of Radio Engineering, Faculty of Electrical Engineering Universiti Teknologi Malaysia. He is now an Associate Professor at Universiti Teknologi Malaysia. His research interest includes the areas of design of active and passive antennas,dielectric resonator antennas, microstrip antennas, reflectarray antennas Electromagnetic band gap (EBG), artificial magnetic conductors (AMC), lefthanded metamaterial (LHM) and computer aided design for antennas. He has published over 80 Journal articlesand conferences paper. He received the gold medal for his invention at Seoul International Invention Fair (SIIF) in 2008 and 2009. Dr. Mohamad Kamal is a senior member of IEEE since 2007. He is a member of Antennas and Propagation Society and Microwave Theory and Technique